NASA Technical Memorandum 81894

NASA-TM-81894 19810007920

SOLAR-PUMPED GAS LASER DEVELOPMENT

John W. Wilson

DECEMBER 1980

NASA
National Aeronautics and
Space Administration

Langley Research Center
Hampton, Virginia 23665

Table of Contents

NOMENCLATURE

Symbols:

a, ℓ	- characteristic interaction length, cm
A	- electromagnetic potential operator, eV - spontaneous decay rate, sec^{-1} - projected area, cm^2 - density of species A, cm^{-3}
B	- photon resonant absorption coefficient, cm^3/sec - density of species B, cm^{-3}
c	- speed of light, cm/sec - van der Waal's constant, eV-cm
C	- solar concentration
d	- oscillator amplitude, cm
e	- unit electric charge, coulombs
E	- energy, eV
E1	- electric dipole transition moment, cm
E2	- electric quadrupole transition moment, cm
E_e	- electronic excitation energy, eV
E_r	- rotational energy, eV
E_T	- energy transferred, eV
$F^{(1)}$	- momentum-coupled transition energy, eV
$F^{(2)}$	- spin-coupled transition energy, eV
$F(\lambda)$	- fractional absorption
$g(\nu)$	- line shape factor
g_λ	- multiplicity of state λ
h	- Planck's constant, eV-sec
H_{ke}	- kinetic energy operator, eV
H_{int}	- interaction hamiltonian, eV
I	- moment of inertia, g - cm^2
$I(\nu)$	- photon intensity, eV/cm^2-sec-μm

j - electronic angular momentum (quantum number)

J - molecular angular momentum (quantum number)

k - Boltzman's constant, eV/°C
- photon wave number, cm^{-1}

K - gas kinetic collision rate coefficient, cm^3/sec

K_{vv} - vibration-to-vibration energy transfer coefficient, cm^3/sec

K_r - effective two-body recombination coefficient, cm^3/sec

L - absorbing path length, cm

m_i - mass of the i particle, g

M - density of molecular species, cm^{-3}

M^* - density of electronically excited molecular species, cm^{-3}

M - density of vibrationally excited molecular species, cm^{-3}

$M1$ - magnetic dipole transition moment, cm

N - number density of molecular species, cm^{-3}

N_λ - number density of state λ, cm^{-3}

O_i - higher order terms

p - pressure, kPa

P - momentum operator, eV/c

q - quenching rate coefficient, cm^3/sec

Q - quenching rate, sec^{-1}

$R_{\lambda\mu}$ - dipole transition moment, cm

s - spin quantum number

S - total spin operator

S_1 - primary photoabsorption rate, sec^{-1}

t - time, sec

T - gas temperature, °K

T_v - vibrational temperature, °K

v	- gas molecular speed, cm/sec
V	- intramolecular potential energy, eV - volume, cm^3
W	- photon emission rate, cm^3/sec - photon absorption rate, cm^3/sec
x	- position, cm
Z_p	- number of collisions before process P occurs
α	- gain coefficient, cm^{-1}
Γ	- line width, sec^{-1}
Δ	- difference operator
ϵ	- photon polarization state
η	- vibrational energy dilution factor
θ	- scattering angle, rad
Θ_r	- rotational quantum, °K
Θ_v	- vibrational quantum, °K
κ_v	- photon attenuation coefficient, cm^{-1}
λ	- photon wavelength, cm - state quantum number
μ	- state quantum number
$\mu(\lambda)$	- photon attenuation coefficient, cm^{-1}
ν	- vibration quantum - photon frequency, sec^{-1} - oscillator frequency, sec^{-1}
π_j	- state j parity value
$\rho(\nu)$	- photon density, cm^{-3}/sec
σ	- cross section, cm^2 - Pauli spin operator
T_e	- period associated with electronic transition, sec
T_{int}	- interaction time, sec
T_N	- vibration equilibration time, sec

T_V - vibration period, sec

τ_λ - lifetime of state λ, sec

$\phi(\lambda)$ - photon flux, cm^{-2} sec^{-1} μm^{-1}

ω_0 - vibrational energy quantum, eV

Subscripts:

E - electronic

E-E - electronic-to-electronic transfer

E-T - electronic-to-translational transfer

E-V - electronic-to-vibrational transfer

r - rotational

R-T - rotational-to-translational transfer

T - translational

T-T - translational-to-translational transfer

V - vibrational

V-T - vibrational-to-translational transfer

V-V - vibrational-to-vibrational transfer

$\lambda\mu$ - λ-to-μ transitions

Superscripts:

* - electronically excited

† - vibrationally excited

SOLAR-PUMPED GAS LASER DEVELOPMENT

John W. Wilson
Langley Research Center

SUMMARY

High power lasers in space have potential as an effective means of space power transmission. The direct conversion of solar radiation into an inverted population for extraction in an optical cavity holds promise as a relatively simple system design when compared to other means of producing laser power through intermediate energy conversion steps. A survey of gas properties through detailed kinetic models has led to the identification of critical gas parameters for use in choosing appropriate gas combinations for solar-pumped lasers. Broadband photoabsorption in the visible or near-UV range is required to excite large volumes of gas and to insure good solar absorption efficiency. The photoexcitation density is independent of the absorption bandwidth. The state excited must be a metastable state which is not quenched by the parent gas. The emission bandwidth must be less than ~ 10 Å to insure lasing threshold over reasonable gain lengths. The system should show a high degree of chemical reversibility and an insensitivity to increasing temperature. Other properties such as good quantum efficiency and kinetic efficiency are also implied. Although photoexcitation of electronic-vibrational transitions is considered as a possible system if the emission bands are sufficiently narrow, it appears that photodissociation into atomic metastables is more likely to result in a successful solar-pumped laser system.

INTRODUCTION

High power lasers have been suggested as a convenient means of space power transmission (ref. 1). As a result, much of the advanced work in energetics for space use is concerned with laser energy conversion. Although the conversion of electrical energy to laser output is considered possible with present technology using photovoltaic devices as the means of electrical power generation, a more direct scheme for conversion of solar radiation to laser output is more attractive due to design simplification, increased reliability, and potentially (relatively) high conversion efficiency (ref. 2).

The first solar-pumped laser utilized a solid state system (ref. 3) which is adequate for use in communications but is unsuited for high power continuous operation due to the slow cooling rate. Continuous high power requires the use of gaseous or liquid systems. The first proposed solar-pumped gaseous laser (ref. 2) uses the atomic iodine inversion obtained by photodissociation of the perfluoroakyliodides. Such a system appears feasible and competitive with other means of space power transmission. It is mainly limited by the solar absorption efficiency in its operation (refs. 2 and 4). Work towards experimental verification is in progress (ref. 5).

It is now of interest to identify other gases which may be utilized as solar lasers for which there is a better match to the solar spectrum and high quantum efficiency. Considered herein are the basic kinetic processes and the range of rate constants for energy handling of various gases and gas combinations. It is the purpose herein to identify critical gas properties to help guide the choice for candidate gases for testing as solar-pumped space lasers.

BASIC KINETIC PROCESSES

The gas kinetic collision rate for neutral gas molecules is taken as

$$K = \langle v\sigma \rangle \approx 2 \times 10^{-10} \text{ cm}^3/\text{sec} \tag{1}$$

according to values in Table I for T = 300°K (ref. 6). Energy is transferred in such processes, the rate of which depends on the type of energy and the collision partners.

Translational Relaxation

The high translational energy (1 to 3 eV) of a hot molecule transfers its energy by the amount

$$E_T = \frac{2m_1 m_2 E}{(m_1 + m_2)^2} (1 + \cos\theta) \tag{2}$$

where m_1 and m_2 are the masses of the two colliding molecules, E the initial energy, and θ is the center-of-mass scattering angle. For isotropic scattering, one-half the energy is transferred per collision in a typical gas ($m_1 \approx m_2$) so that a very hot molecule is cooled in

$$Z_{T-T} \approx \ln (E/kT) < 10 \tag{3}$$

collisions where T is the gas temperature.

Rotational Relaxation

The rotational energy of a diatomic molecule is

$$E_r = \frac{h^2 J(J+1)}{2I}$$

$$= k\Theta_r J(J+1) \tag{4}$$

where J is the rotational quantum number, I is the moment of inertia, and Θ_r has units of temperature. Selection rules for homonuclear rotational changing collisions is $\Delta J = 2$. The rotational energy change is then

$$\Delta E_r = 4k\Theta_r \left(J - \frac{1}{2}\right) \tag{5}$$

The value of Θ_r for H_2 is 85°K so that for $J \geq 2$

$$\Delta E_r \geq k\,(510°K) \tag{6}$$

for which rotational changes are expected to be slow (ref. 7) except at high gas temperatures ($T \gg 510°K$). This is expected for all hydrogenic molecules combined with only one heavier atom. Rotational changes for most other molecules are expected to occur rapidly due to their much larger moment of inertia (table I).

Models of diatomic relaxation assuming the rotating molecule interacts through central forces located at each nuclei with the colliding molecule have been applied to H_2 using perturbation theory with good success. However, in application to molecules with large moments of inertia, the perturbation theory breaks down so that little success has been achieved. Values of rotation relaxation (ref. 7) are given in table II, and it is generally seen that rotational relaxation occurs in

$$Z_{R-T} < 100 \tag{7}$$

collisions except for the hydride molecules.

Vibrational Relaxation

Insight is gained on vibrational relaxation by considering Ehrenfest's principle. If the interaction time in collision with a vibrating system is long compared to the oscillator period, then the quantum numbers of the periodic motion are left unchanged by the interaction. Comparing the oscillator period τ_v with the time of interaction τ_{int} as

$$\frac{\tau_{int}}{\tau_v} \approx \frac{a}{\pi d} \left(\frac{\Theta_v M_1}{T M} \right)^{\frac{1}{2}} \tag{8}$$

where a is the interaction distance, d is the oscillator amplitude, $h\upsilon = k\Theta_v$ is the unit of oscillator quantum energy, kT the background gas kinetic energy, M_1 the mass of the colliding molecule, and M the reduced mass of the oscillator (ref. 8). For most molecules, $\Theta_v \gg T$ and $a \gg d$, so that $\tau_{int} \gg \tau_v$ and adiabatic collisions are most common for which vibrational relaxation is very slow.

A simple theory of such collisions was developed by Landau and Teller as a classical analog to the Ehrenfest principle. They found the vibrational relaxation rate of a classical oscillator in collisions with a gas of temperature T as

$$Z_{V-T} \approx \sqrt{\frac{3}{2\pi}} \left(\frac{\Theta_v}{T} \right)^{-\frac{1}{6}} \exp \left[\frac{3}{2} \left(\frac{\Theta_v}{T} \right)^{\frac{1}{3}} \right] \tag{9}$$

The dominant dependence of the exponential is clearly displayed in the experimental data. Vibrational relaxation data are given for a number of gases (refs. 7 and 9) in table III, and gas combinations (refs. 7, 9, and

10) in table IV and the slowness of vibrational relaxation is clearly seen. The relatively rapid relaxation of CO by atomic oxygen displayed in table IV is apparently due to the formation of a carbon dioxide complex as

$$CO(1) + O \longrightarrow CO_2^* \longrightarrow CO + O \tag{10}$$

A model for this reaction appears not available. Similarly for the triatomics, we see

$$CO_2 + H_2O \longrightarrow H_2CO_3 \longrightarrow CO_2 + H_2O \tag{11}$$

as a de-excitation mechanism (ref. 9).

Electronic Excitation Relaxation (Quenching)

We again examine the question of adiabaticity of background collisions with excited states. The period of the transition oscillation of the electronic state is

$$\tau_e = h / E_e \tag{12}$$

while the interaction time is taken as before to be

$$\tau_{int} = a / v \tag{13}$$

where a is the range of the interaction and v is the relative velocity. When the interaction is not between strongly attractive atoms or molecules, then the interaction time is evaluated at gas kinetic velocities for which

$$\tau_{int} \approx 5 \times 10^{-8}/2 \times 10^{4} \approx 2 \times 10^{-12} \text{ sec} \tag{14}$$

so that the adiabatic region is defined as

$$E_e >> h/\tau_{int} \approx 2 \times 10^{-3}. \tag{15}$$

Hence, energetic ($E_e > 0.5$ eV) electronic states will generally de-excite slowly provided the states are not chemically active (refs. 8 and 9).

In the event of collision between chemically active species, then the interaction velocity appropriate to the adiabatic condition is that associated with the potential well depth as

$$v \approx \sqrt{\frac{2V}{M_1}} \approx 10^5 \text{ cm/sec} \tag{16}$$

where V is the well depth and M_1 the reduced mass. It follows that the adiabetic condition is

$$E_e >> 2 \times 10^{-2} \text{ eV}. \tag{17}$$

The adiabaticity is lost for the lowest spin-orbit coupled levels with energy below a tenth of an electron volt. However, there is generally poor coupling between the translational and electronic states and this coupling is further hindered as the electronic transition energy increases. If additional internal degrees of freedom exist within the colliding systems, then the effective mismatch between electronic and translational energy can be reduced with a corresponding increase in quenching rates. For example, H_2 with its small moment of inertia is often a notably more effective quencher due to electronic to rotational coupling terms as seen in table V. Unusually efficient transfers may be caused by vibration excitation which is the case for

$$Fe(a^5D_3) + CO \longrightarrow Fe(a^5D_4) + CO(_1) \qquad (18)$$

Other cases which are clearly promoted by E-V transfers are discussed in the next section. The efficiency of

$$Fe(a^5D_3) + Fe \longrightarrow Fe(a^5D_4) + Fe \qquad (19)$$

may well be due to an intermediate complex being formed. The data in table V are shown in figure 1 where the values affected by internal energy transfer and complex formation are shown as asterisks. The line is taken as the value of strict transfer of electronic to translational energy.

It has already been noted that E-R transfers in the case of H_2 and D_2 are effective for quenching low-lying electronic states. Other hydrides probably play the same role due to their small moment of inertia. We have also suggested that chemical complex formation is important. In many cases of complex formation, a fraction of the energy is handed over to vibration levels and will be discussed in a subsequent section.

It is suggested by Hoffman and Leone (ref. 11) that the quenching of $Br(4^2P_{1/2})$ by the halogens and interhalogens is by an intermediate triatomic complex which dissociates into quenched states. The $I(5^2P_{1/2})$ is probably similarly deactivated. Values are given in table VI. The approximate values for $I(5^2P_{1/2})$ are judged on the basis of the strengths of the trimolecular interhalogen complexes formed (ref. 11).

The quenching of $I(5^2P_{1/2})$ by iodine-substituted organic molecules has been extensively studied in connection with atomic iodine laser development (ref. 12). Quenching rates are given in table VII. The importance of steric factors is to be noted in the two measurements for propyliodide.

Electronic-to-Vibrational Excitation Transfer

Already mentioned in regard to spin-orbit relaxation was the role of internal rotational energy of H_2 and D_2. Transfer to vibrational levels can also facilitate spin-orbit relations as noted by examples (ref. 9) in table VIII.

The spin-orbit relaxation of the $Hg(6^3P)$ levels with molecules is also observed (ref. 9) as

$$Hg(6^3P_1) + N_2(0) \longrightarrow Hg(6^3P_0) + N_2(v = 1) \quad (20)$$

Further spin-orbit relaxation data (ref. 9) are shown for other molecules in figure 2.

Another example is the atomic halide metastable. It is presumed that $I(5^2P_{1/2})$ transfers in chemical exchange reactions (ref. 9) as

$$I(5^2P_{1/2}) + H_2 \longrightarrow IH(v) + H \quad (21)$$

$$I(5^2P_{1/2}) + C_3H_8 \longrightarrow HI(v) + C_3H_7 \quad (22)$$

as examples. No information is known as to the possible vibrational levels reached. The $Br(4^2P_{1/2})$ metastable undergoes similar reactions (refs. 11 and 13) as undoubtedly do the other halides. The halides also undergo other E-V transfer reactions (refs. 9, 13 to 17) as

$$I(5^2P_{1/2}) + N_2 \longrightarrow I(5_2P_{3/2}) + N_2(v = 3) \quad (23)$$

$$Br(4^2P_{1/2}) + CO_2 \longrightarrow Br(4^2P_{3/2}) + CO_2(1,0,1). \quad (24)$$

The exact mechanism of the transfer has not been studied, but may involve intermediate vibrationally excited ionic states resulting from the halide electronegativity. Table IX lists quenching for halide metastables without reference to the final states populated. Table X gives the corresponding coefficients for specific reaction channels. Many other halogen metastable E-V transfers have been observed, but rates have not always been estimated.

The role of curve crossing with ionic states is clearly seen in the electronic relaxation of the alkali metals (ref. 18). The first observed example (ref. 9) was that for $Na(3^2P)$ relaxation to $Na(3^2S)$ by vibrational excitation of N_2. Electronic to vibration transfer seems most efficient in the v = 3-4 levels for H_2, D_2, CO, N_2, and C_2H_4. The transfer to O_2, CO_2, and N_2O seems to require near-resonant transfer. Values for $Na(3^2P)$ quenching (ref. 9) are given in table XI. Similarly rapid E-V transfer is observed and predicted for the other alkali metals (ref. 18). Quenching rates for spin-orbit relaxation in thallium is shown in table XII.

Excitation transfer for $O(2^1D_2)$ to O_2, N_2, and CO appears through an intermediate triatomic complex (ref. 13) as

$$O(2^1D_2) + O_2 \longrightarrow O_3^* \longrightarrow O(2^3P_J) + O_2(v) \quad (25)$$

Rates (ref. 19) are given in table XIII.

The transfer of electronic excitation of some molecules is on the order of that for atomic transfer. Experimental observation has been made for (ref. 13)

$$CO(d^3\Delta)_{v=7} + CO \longrightarrow 2CO(v) \quad (26)$$

$$CO(a^3\pi) + CO \longrightarrow 2CO(v) \tag{27}$$

$$O_2(^1\Delta g) + NO \longrightarrow O_2 + NO(v) \tag{28}$$

and others. Reaction rates (ref. 19) are given in table XIV.

Electronic-Electronic Excitation Transfer

Suppose now that two oscillator systems interact with one initially excited with frequency ν_1 and the other unexcited with frequency ν_2. The beat frequency $\nu_1 - \nu_2$ is related to the energy separation between the states

$$\Delta E = h(\nu_1 - \nu_2). \tag{29}$$

The efficiency with which the energy associated with beat can be extracted is estimated by the Ehrenfest principle and requires

$$\Delta E \ll h / \tau_{int} \approx h\, v/\ell \approx 0.01 \text{ eV} \tag{30}$$

where the interaction distance $\ell \approx 10^{-8}$ cm and the velocity at collision $v \approx 2 \times 10^4$ cm/sec. Excitation transfer for allowed atomic transitions seem to follow

$$Z_{E\text{-}E} \sim \exp\left(\frac{\Delta E}{3h / \tau_{int}}\right). \tag{31}$$

The dipole-dipole transfer seems to be long-ranged so that (for $\Delta E = 0$)

$$Z_{dipole\text{-}dipole} \approx 1. \tag{32}$$

whereas transfer among quadrupole transitions is slower as

$$Z_{quad\text{-}quad} \approx 10 - 100. \tag{33}$$

Energy transfer requiring spin vector changes are quite slow as

$$Z_{\Delta s} \approx 10^3. \tag{34}$$

Transfer of atomic electronic energy to molecular electronic energy is further governed by the Franck-Condon principle. Spin conservation rules are still appropriate in many cases although there are also many exceptions. Values (ref. 20) for transfer from $Ar(^3P_1)$ and $Ar(^1P_1)$ to several molecules are given in table XV. Further values (ref. 20) for the transfer of molecular electronic energy among molecules is given in table XVI for $N_2(A^3\Sigma_u)$ metastables.

Although the estimates of equations (32) to (33) describe trends in the data, there are notable exceptions. Even so, equations (31) to (34) are reasonable starting values for systems which are otherwise unknown.

Vibration-Vibration Transfer

There are two mechanisms for bringing about transfer of vibrational energy from one molecule to another. If the levels are in near resonance, then efficient transfer can occur through a long-range dipole-dipole interaction or dipole-quadrupole interaction if dipole transitions are disallowed for one of the collision partners (ref. 21). These long-range processes are inhibited when the energy excess satisfies

$$\Delta E >> .02 \text{ eV} \tag{35}$$

so that the short-range repulsive interaction of the molecules becomes the dominant vibration transfer process (see fig. 3). Calculations of Jeffers and Kelley (ref. 21) are shown in comparison to experimental values for CO relaxation in CO. Further values (ref. 10) for CO are shown in table XVII. Additional values (ref. 9) for assorted molecules are given in table XVIII.

Summary

We now summarize the values of the several reaction types and their ranges of validity. A hot molecule (high translational energy) is thermalized in

$$Z_{T-T} \leq 10 \tag{36}$$

collisions. High rotational energy is transferred in

$$Z_{R-T} \leq 100 \tag{37}$$

collisions while high vibrational energy is transferred in

$$10^2 \leq Z_{V-T} \leq 10^9 \tag{38}$$

collisions. The lower limit on Z_{V-T} applies when some complex is formed in the process. Otherwise, helium and H_2 are most efficient gases for vibrational cooling requiring 10^5 collisions. This usually poor coupling between vibrational and translational motions means that vibrational temperatures approach background gas temperatures very slowly. Vibrational energy is transferred among near resonance levels in

$$10 \leq Z_{V-V} \leq 10^4 \tag{39}$$

collisions. The lower limit applies when a permanent dipole moment exists in both molecules. Since vibrational energy is rapidly shared among near-resonant vibrational levels, nonequilibrium gases will often have R-T equilibrium at one temperature with vibrational equilibrium at a quite different temperature. The transfer of electronic energy to translational motion is generally slow

$$10^4 \leq Z_{E-T} \leq 10^6 \tag{40}$$

unless an intermediate complex is formed with curve crossing to unexcited levels or the excited level is on the order of thermal energies for which

$$10 \leq Z_{E-T} \leq 100. \tag{41}$$

The transfer of electronic excitation to low vibrational levels can occur near resonance in only a few collisions. Off resonant or transfer to high vibrational states is much slower so that

$$2 \leq Z_{E-V} \leq 10^6. \tag{42}$$

Transfer of electronic energy to other electronic states can be very efficient near resonance (lower limit)

$$1 \leq Z_{E-E} \leq 10^6 \tag{43}$$

but is otherwise quite slow (upper limit). Selection rules are also important in such energy transfer.

The important energy handling processes being summarized in equations (36) to (43), we now proceed to study the gas coupling to the radiation field of the solar radiance and the fluorescence of the gas.

RADIATION COUPLING

Atomic and molecular systems interact with electromagnetic radiation through internal currents and charges. The proper description is through minimal electromagnetic coupling in which the individual particle momentum operator P is replaced by

$$P \longrightarrow P - \frac{e}{c} A \tag{44}$$

where A is the electromagnetic potential operator (refs. 22 and 23). The appropriate kinetic energy operator (ref. 23) is

$$H_{ke} = \frac{\boldsymbol{\sigma} \cdot P \quad \boldsymbol{\sigma} \cdot P}{2m} \tag{45}$$

in classical quantum theory in which σ is the appropriate spin operator. The interaction potential then follows as

$$H_{int} = \sum_n \left\{ \frac{-e}{2mc} \left[P_n \cdot A(x_n) + A(x_n) \cdot P_n \right] \right.$$

$$+ \frac{e^2}{2mc^2} A(x_n) \cdot A(x_n)$$

$$\left. - \frac{e}{2mc} \sigma_n \cdot [\nabla_n \times A(x_n)] \right\} \tag{46}$$

where, to lowest order, the sum over n includes only the electrons in the system.

Consider the matrix elements between some initial state of the system λ and a final state μ including a photon of wave vector k and polarization ϵ

$$\langle \lambda | H_{int} | \mu \; k \; \epsilon \rangle$$

$$= - \frac{e}{m} \left(\frac{2\pi}{kV} \right)^{\frac{1}{2}} \left\{ F^{(1)} - i F^{(2)} \right\} \tag{47}$$

where

$$F^{(1)} = \langle \lambda | \sum_n \epsilon \cdot P_n \; e^{ik \cdot x_n} | \mu \rangle \tag{48}$$

$$F^{(2)} = \langle \lambda | \sum_n \epsilon \cdot (k \times S_n) \; e^{ik \cdot x_n} | \mu \rangle \tag{49}$$

where S_n is the spin operator. Consider now the expansion of

$$e^{ik \cdot x_n} \quad 1 + ik \cdot x_n - \frac{1}{2} (k \cdot x_n)^2 + \ldots \tag{50}$$

the magnitude of

$$(k \cdot x_n) \approx \frac{1}{\lambda} a \approx \frac{1\text{Å}}{5000\text{Å}} \tag{51}$$

in the region of optical radiation where a is the order of atomic and molecular dimension ($\sim$1 Å). Therefore the exponential converges rapidly for optical transitions. Making an expansion for $F^{(1)}$ and $F^{(2)}$ we have

$$F^{(1)} = \langle\lambda| \sum_n \epsilon \cdot P_n |\mu\rangle + \langle\lambda| \sum_n \epsilon \cdot P_n \, k \cdot x_n \, |\mu\rangle + O_1 \tag{52}$$

$$F^{(2)} = \langle\lambda| \sum_n \epsilon \cdot (k \times S_n) \, |\mu\rangle + O_2 \, . \tag{53}$$

We now make the following simplifications. The operator

$$(\epsilon \cdot P_n)(k \cdot x_n) = \frac{1}{2} [(\epsilon \cdot P_n)(k \cdot x_n) + (\epsilon \cdot x_n)(k \cdot P_n)]$$

$$- \frac{1}{2} (k \times \epsilon) \cdot L_n \tag{54}$$

from which we identify

$$E1 = \langle\lambda| \sum_n \epsilon \cdot P_n |\mu\rangle \tag{55}$$

$$M1 = \langle\lambda| \sum_n (k \times \epsilon) \cdot (L_n + 2S_n) \, |\mu\rangle \tag{56}$$

$$E2 = \frac{1}{2} \langle\lambda| \sum_n [(\epsilon \cdot P_n)(k \cdot x_n) + (\epsilon \cdot x_n)(k \cdot P_n)] \, |\mu\rangle \tag{57}$$

where E1, M1, and E2 are the electric dipole, magnetic dipole, and electric quadrupole transition amplitudes, respectively. Values for the various multipole transitions depend on the symmetry of the initial and

final states and the average magnitude of dynamic variables. We observe

$$E1 \sim |P_n| \sim 1/a \tag{58}$$

$$M1 \sim |P_{n1}|\,|x_n|/\lambda \sim 1/\lambda \tag{59}$$

$$E2 \sim |P_n|\,|x_n|/\lambda \sim 1/\lambda \tag{60}$$

while the remainders

$$O_1 \sim \frac{1}{a}\left(\frac{a}{\lambda}\right)^2 \sim a/\lambda^2 \tag{61}$$

$$O_2 \sim \frac{1}{\lambda}\left(\frac{a}{\lambda}\right) \sim a/\lambda^2 . \tag{62}$$

Dipole transitions (ref. 24) are allowed for

$$|j_\lambda - j_\mu| \leq 1 \qquad \text{except } j_\lambda + j_\mu = 0 \tag{63}$$

$$\pi_\lambda\,\pi_\mu = -1. \tag{64}$$

The total radiative transition coefficient is

$$A_{\lambda\mu} = \frac{64\pi^4 \nu_{\lambda\mu}^3 |R_{\lambda\mu}|^2}{3h} \tag{65}$$

where

$$R_{\lambda\mu} = e\langle\lambda| \sum_n x_n |\mu\rangle. \tag{66}$$

The radiative lifetime for the state λ is

$$\tau_\lambda = \frac{1}{\sum_\mu A_{\lambda\mu}} . \tag{67}$$

The total lifetime for electric dipole transitions (ref. 25) in the optical region is about 10^{-8} sec.

If the electric dipole moment is zero, then magnetic dipole transitions may yet occur if

$$|j_\lambda - j_\mu| \leq 1 \quad \text{except} \quad j_\lambda + j_\mu = 0 \tag{68}$$

$$\pi_\lambda\,\pi_\mu = +1. \tag{69}$$

The state lifetimes in this case are much longer, typically on the order of 10^{-3} sec. Such transitions are among the so-called forbidden transitions (ref. 25).

If the electric and magnetic dipole moments are both zero, transitions may yet occur if

$$|j_\lambda - j_\mu| \leq 2 \quad \text{except} \quad j_\lambda + j_\mu = 0,1 \tag{70}$$

$$\pi_\lambda \pi_\mu = +1, \tag{71}$$

These electric quadrupole transitions with lifetimes on the order of 1 second are generally slower than magnetic dipole transitions. Higher order multipole transitions are so slow that they are never observed in the optical region. States which decay by M1 and E2 or higher order are called metastable. The lifetimes and decay rates are related to other emission and absorption processes as we will now show.

Einstein Relations

Consider an ensemble of quantized systems (ref. 26) in thermal equilibrium with a photon gas all at temperature T. Let N_λ be the density of systems in state λ and N_μ be the density of systems in state μ. The rate of spontaneous emission from state λ to μ is $A_{\lambda\mu}$. Let $B_{\lambda\mu}$ be the rate coefficient for the resonant emission caused by stimulation by the photon gas so that the total rate of emission from state λ is

$$W_{\lambda\mu} = B_{\lambda\mu}\, \rho(\nu) + A_{\lambda\mu} \tag{72}$$

where $\rho(\nu)$ is the photon density between ν and $\nu + d\nu$. The corresponding resonant absorption rate is given as

$$W_{\mu\lambda} = B_{\mu\lambda}\, \rho(\nu)\,. \tag{73}$$

Since the ensemble is in thermal equilibrium with the photon gas, the number of λ-to-μ transitions must be equal to the number of μ-to-λ transitions

$$N_\lambda W_{\lambda\mu} = N_\mu W_{\mu\lambda} \tag{74}$$

and further satisfy

$$\frac{N_\lambda}{N_\mu} = \frac{g_\lambda}{g_\mu} \exp(-h\nu/kT). \tag{75}$$

Combining these relations with the Planck spectral distribution for the photon gas

$$\rho(\nu) = \frac{8\pi h\nu^3}{c^3} \left(\frac{1}{e^{h\nu/kT}-1}\right) \tag{76}$$

we get (ref. 27)

$$\frac{8\pi h\nu^3}{c^3(e^{h\nu/kT}-1)} = \frac{A_{\lambda\mu}(g_\lambda/g_\mu)}{B_{\mu\lambda}e^{h\nu/kT} - B_{\lambda\mu}(g_\lambda/g_\mu)} \tag{77}$$

which implies

$$B_{\mu\lambda} = B_{\lambda\mu}\, g_\lambda/g_\mu \tag{78}$$

and

$$A_{\lambda\mu} = \frac{8\pi h\nu^3}{c^3}\, B_{\lambda\mu}\,. \tag{79}$$

These same relations follow from detailed balance in the quantum theory from which Planck's law can then be derived by assuming thermal equilibrium among the states of the system (ref. 23).

Nonequilibrium Absorption and Emission

Although the Einstein relations were derived to meet the requirements of thermal equilibrium, the relations follow from detailed balance for which the relations are satisfied only because of the properties of the emitting-absorbing systems and quantum mechanics which describe their dynamic behavior. Let us now consider the intensity of photons $I(\nu)d\nu$ moving through a medium. The attenuation of the beam follows Beer's law

$$I(\nu) = I_0(\nu) \exp(-\kappa_\nu x) \tag{80}$$

which satisfies the transport equation

$$\frac{dI(\nu)}{dx} = -\kappa_\nu I(\nu) \tag{81}$$

where κ_ν is the attenuation coefficient. Alternatively, the change of the photon energy density within a volume element is

$$\begin{aligned}\frac{d[\rho(\nu)d\nu]}{dt} &= h\nu[W_{\lambda\mu}\, dN_\lambda(\nu) - W_{\mu\lambda}\, dN_\mu(\nu)] \\ &= h\nu[B_{\lambda\mu}\,\rho(\nu)\, dN_\lambda(\nu) - B_{\mu\lambda}\,\rho(\nu) dN_\mu(\nu)]\end{aligned} \tag{82}$$

where $dN_\lambda(\nu)$ are the number of systems available for stimulated emission into the frequency interval between ν and $\nu + d\nu$ and $dN_\mu(\nu)$ are the number of absorbers in the same interval. In the time interval dt the wave front will advance a distance

$$dx = c\ dt. \tag{83}$$

Recalling the relation between the intensity and energy density as

$$I(\nu) = c\ \rho(\nu) \tag{84}$$

where c is the velocity of light. Using these quantities in the above relations we have

$$\frac{1}{I(\nu)} \frac{d[I(\nu)d\nu]}{dx} = -\kappa_\nu d\nu$$

$$= \frac{h\nu}{c} [B_{\mu\lambda}\ dN_\mu(\nu) - B_{\lambda\mu}\ dN_\lambda(\nu)] \tag{85}$$

as obtained using equations (81), (82), and (84). After summing over all frequencies

$$\kappa = \int \kappa_\nu\ d\nu = \frac{h\nu_o}{c} [B_{\mu\lambda}N_\mu - B_{\lambda\mu}N_\lambda] \tag{86}$$

where ν_o is the central frequency (ref. 26). It is convenient to define the line shape $g(\nu)$ such that

$$\int g(\nu)\ d\nu = 1 \tag{87}$$

so that the attenuation coefficient is

$$\kappa_\nu = \kappa g(\nu)$$

$$= \frac{h\nu_o}{c} B_{\mu\lambda} [N_\mu - \frac{g_\lambda}{g_\mu} N_\lambda]\ g(\nu). \tag{88}$$

We further define the absorption cross section as

$$\sigma_{abs}(\nu) = \frac{h\nu_o}{c} B_{\mu\lambda}\ g(\nu) \tag{88}$$

or alternatively

$$\sigma_{abs} = \frac{c^2 A_{\lambda\mu}}{8\pi \nu_o^2}\ g(\nu)$$

$$= \frac{\lambda_o^2 A_{\lambda\mu}}{8\pi}\ g(\nu). \tag{90}$$

Similarly the stimulated emission cross section

$$\sigma_{se}(\nu) = \frac{\lambda_o^2 A_{\lambda\mu}}{8\pi} \frac{g_\mu}{g_\lambda} g(\nu) \tag{91}$$

where λ_o is the central wavelength.

Line Shape and Broadening

There are several factors which contribute to the width of a spectral line. A most fundamental contribution is that due to radiation damping arising from the interaction of the emitting system with its own radiation (ref. 28). The line shape for the decay of such an isolated system was derived by Lorentz and was found to exhibit what is now known as the Lorentz profile as

$$g(\nu) = \frac{\Gamma}{2\pi} \frac{1}{(\nu-\nu_o)^2 + (\Gamma/2)^2} \tag{92}$$

where Γ is the decay constant and therefore identified with the Einstein A coefficient for the transition. These same conclusions follow from a quantum treatment of the same problem as given in reference 29. The bandwidths in the optical region are therefore

$$1 < \Delta\nu < 10^8 \text{ sec}^{-1} \tag{93}$$

corresponding to wave-length dispersion of

$$10^{-15} < \Delta\lambda < 10^{-6} \ \mu\text{m} . \tag{94}$$

These widths are appropriate for atomic and molecular vibrational-rotational transitions of isolated systems at rest.

The frequency shift of an oscillator in relative motion to an observer is

$$\frac{\nu - \nu_o}{\nu_o} = \frac{v}{c} \tag{95}$$

where v is the relative velocity component. The average frequency shift for a gas in thermal equilibrium at temperature T is

$$\frac{\nu - \nu_o}{\nu_o} = \frac{1}{c}\sqrt{\frac{kT}{2m}} \tag{96}$$

yielding a bandwidth of

$$\Delta\nu \approx 10^9 \text{ sec}^{-1} \tag{97}$$

at room temperature. The corresponding wavelength dispersion is

$$\Delta\lambda \approx 10^{-5} \text{ μm}. \tag{98}$$

This Doppler broadening of the transition line is the limiting resolution for most atomic optical transitions.

A particularly lucid discussion of the effects of collisions on a radiating system in terms of random phase change is given by Siegman (ref. 30). Assuming a collision results in a uniformly distributed and completely random phase change at the collison rate ν_{coll} then the transition with decay rate A is found to have a Lorentz line shape with

$$\Gamma = A + 2\,\nu_{coll}. \tag{99}$$

The line broadening due to collisions is then

$$\Delta\nu = 2\,N\,K$$

$$\approx 10^8\,p \tag{100}$$

where N is the gas density and p is the pressure in kPa. The wavelength dispersion at standard conditions for optical transitions is

$$\Delta\lambda \approx 10^{-4} \text{ μm} \tag{101}$$

and therefore dominates the line width at standard conditions.

At sufficiently high pressure the radiating systems are in close proximity with surrounding gas molecules and are generally in some quasi-molecular state (i.e., van der Waals binding). Collisions of this type, in distinction to collisions leading to random phase change, are noncentral and at no point is their relative velocity zero. The transition frequency then corresponds to the separation of the two potential curves at the relative nuclear separation at which the transition occurred in accordance with the Franck-Condon principle (ref. 31). The frequency shift is related to the separation as

$$\Delta\nu = \frac{|c' - c''|}{r^6} \tag{102}$$

where c' and c'' are the potential constants of the two levels for the van der Waals potential of $-c/r^6$. Note that the level shift is asymmetrically shifted toward either red or blue depending on the relative magnitudes of c' and c''. The level shift is nearly proportional to the line width and depends on pressure as

$$\langle r \rangle \sim 1/p^{1/3} \tag{103}$$

so the line width is approximately

$$\Delta\nu \sim |c' - c''| \; p^2. \tag{104}$$

Corresponding line shifts of

$$\Delta\lambda \approx 10^{-4} \; \mu m \tag{105}$$

have been observed in some cases.

Similar to the van der Waals broadening is the electronic transitions in molecules. The transition is governed by the Franck-Condon principle for which the frequency of the radiation is related to the difference between the potential curves

$$\nu = V''(r) - V'(r) \tag{106}$$

where r is the appropriate nuclear separation which varies according to the vibrational state of the molecule. Within the uncertainty of the nuclear separation (given by the wavelength of the vibrational motion) there is a corresponding uncertainty in the transition frequency

$$\Delta\nu = \frac{dV'(r)}{dr} \; \lambda_{vib} \tag{107}$$

where λ_{vib} is the vibrational wavelength and has the range

$$10^{-6} < \lambda_{vib} < 5 \times 10^{-3} \mu m. \tag{108}$$

The line width is correspondingly

$$3 \times 10^{10} < \Delta\nu < 1 \times 10^{13} \; sec^{-1} \tag{109}$$

and the wavelength dispersion

$$10^{-4} \leq \Delta\lambda \leq 4 \times 10^{-2} \mu m \tag{110}$$

where the lower value corresponds to weak van der Waals molecules.

The energy handling processes discussed in the previous section and the radiation coupling of the present section are the principal processes by which light is absorbed, processed, and emitted by gaseous systems. Subsequent sections will discuss the potential for such gases absorbing light from thermal or solar sources in order to form a sufficient population inversion to cause oscillation in a properly designed optical cavity.

LIGHT ABSORPTION FROM A THERMAL SOURCE

The thermal irradiance $I(\lambda)d\lambda$ at the surface of a source at temperature T is related to the photon flux $\phi_0(\lambda)d\lambda$ as

$$I(\lambda)d\lambda = \varepsilon_\lambda \, \phi_0(\lambda)d\lambda \tag{111}$$

where ε_λ is the photon energy and

$$\phi_0(\lambda) = \frac{2\pi c}{\lambda^4} \frac{1}{\exp\,(hc/k\lambda T) - 1} \tag{112}$$

where $hc/k = 1.44$ cm-deg. The irradiance for a point source reduces for increasing distance according to Gauss' Law. The fractional absorption in a gas-filled collector is given as

$$F(\lambda) = 1 - \exp\,[-\mu(\lambda)\, L] \tag{113}$$

where $\mu(\lambda)$ is the attenuation coefficient for the gas and L is related to the collector geometry. It is clear in comparing with equation (80) that $\mu(\lambda)$ numerically equals κ_ν at the appropriate frequency ν.

Consider the simple geometry of normal incidence on a layer of gas of thickness L. The total number of photons absorbed is

$$\Delta N_\gamma = A \int F(\lambda) \quad \phi_0(\lambda)d\lambda \tag{114}$$

where A is the frontal area of the layer. The number of photons absorbed per unit volume of material is

$$\frac{\Delta N_\gamma}{\Delta V} = \frac{1}{L} \int \quad F(\lambda) \; \phi_0(\lambda)d\lambda \,. \tag{115}$$

The attenuation coefficient is found from the photoabsorption cross section given by equation (90) as

$$\mu(\lambda) = \frac{\lambda_a^2 \quad A_a}{8\pi} g_0(\nu) \; N_0 \tag{116}$$

where λ_a is the central wavelength, A_a is the Einstein coefficient for the decay of the excited state formed, $g_0(\nu)$ is the appropriate line-width function, and N_0 the gas density. Taking L to be on the order of $\mu(\lambda_a)^{-1}$ we find

$$\Delta N_\gamma \approx A \; \phi_0(\lambda_a) \; \Delta\lambda_a \tag{117}$$

and

$$\frac{\Delta N_\gamma}{\Delta V} \approx \mu(\lambda_a) \; \phi_0(\lambda_a)\Delta\lambda_a \tag{118}$$

where (92) and (118) yield

$$\frac{\Delta N_\gamma}{\Delta V} \approx \frac{\lambda_a^4 A_a}{4\pi^2 c} \quad \Phi_o(\lambda_a) N_o \tag{119}$$

with

$$\Delta \nu_a = \frac{c}{\lambda_a^2} \Delta\lambda_a . \tag{120}$$

The main result is that the total number of excited states formed in a "good" collector depends on the bandwidth of the absorption line, while the density of excited states found in the gas is dependent on the central wavelength λ_a and the strength of the transition moment as reflected in the value of A_a and is independent of the bandwidth.

SOLAR ABSORPTION

The photoabsorption cross section is given by

$$\sigma_a = \frac{\lambda^2_a A_a}{4\pi^2 \Delta\upsilon_a} \tag{121}$$

where λ_a is the central wavelength, A_a is the Einstein coefficient, and $\Delta\nu_a$ is the line width. Using

$$\Delta\nu_a = \frac{c}{\lambda_a^2} \Delta\lambda_a \tag{122}$$

we obtain the photoexcitation rate coefficient as

$$S_1 = \sigma_a \quad \phi_s(\lambda_a)\ \Delta\lambda_a$$

$$= \frac{\lambda^4_a\ A_a}{4\pi^2 c} \quad \phi_s(\lambda_a) \tag{123}$$

where $\phi_s(\lambda_a)$ is the concentrated solar irradiance of the gas at the central wavelength λ_a. The solar irradiance is bound by its peak value at $\lambda_a \approx 5000$A (ref. 32)

$$\phi_s(\lambda_a) \leq 6 \times 10^{21}\ C\ (\gamma/cm^2\text{-cm-sec}) \tag{124}$$

where C is the solar concentration. We have then

$$S_1 \leq 3.3 \times 10^{-8}\ A_a\ C\ (sec^{-1}) \tag{125}$$

If the solar absorption process raises the groundstate molecule M to an electronically excited vibrational state M^* as

$$M + \gamma_s \longrightarrow M^*\ (\upsilon) \tag{126}$$

the final states $M^*(\upsilon)$ are approximately normally distributed in υ over a width $\Delta\upsilon$ about some $\bar{\upsilon}$. The $\Delta\upsilon$ and $\bar{\upsilon}$ are found through the Franck-Condon factors. It often occurs that the photoabsorption dissociates the molecule into two fragments only one of which is electronically excited.

KINETIC MODEL OF E-V LASER

Photon absorption in a molecular gas through an electronic transition is governed by the Franck-Condon principle for which the nuclear separations are relatively fixed, but the interaction potential undergoes a radical change as indicated by the vertical dashed lines in figure 4. The photon energy at which maximum absorption occurs is the energy difference between the two potential curves at the most probable nuclear separation of the ground state vibrational wave function as indicated by the central-vertical-dashed line in figure 4. The most probable vibrational mode after absorption is $\bar{v} \approx 13$ as indicated in the figure. The photoabsorption frequency range as well as the range of vibrational levels reached $\Delta v \approx 6$ are determined by the ground state vibrational wave functions' width as indicated in the figure.

The vibrational excitation of the upper vibrational levels are shared among one another through

$$M^*(v) + M^*(v') \longrightarrow M^*(v - 1) + M^*(v' + 1). \tag{127}$$

Transfers such as

$$M^*(v) + M(0) \longrightarrow M^*(v - 1) + M(1) \tag{128}$$

generally do not occur since the vibrational level spacing among the electronic excited state do not match those of the groundstate vibrational levels.

The excited states are initially produced with an average vibrational level $\bar{v}$. Through collisions among themselves, they will relax to an equilibrium distribution at temperature

$$T_V \approx \bar{v}\,\omega_0/k \tag{129}$$

where ω_0 is the energy spacing between levels. Approximately $\bar{v}$ such collisions are required before equilibrium is achieved. Initially the molecules are produced with a (approximately) normal distribution in vibrational levels centered at $\bar{v}$ and of width Δv. There is a continuous progression from this initial normal distribution towards the equilibrium. The extent of the progression depends on the ratio of the lifetime of the electronic state to the equilibration time of the vibrational levels.

The equilibration time can be greatly reduced by adding a second gas N for which V-V resonance is established such that

$$M^*(v) + N(o) \longrightarrow M^*(v-1) + N(1) \tag{130}$$

occurs frequently. The additional effect of such a second gas is that the equilibrium temperature is greatly reduced to

$$T_V = \eta \frac{\bar{v}\,\omega_0}{k} + (1 - \eta)T_g \tag{131}$$

where T_g is the background gas temperature and

$$\eta = \frac{M^*}{M^* + N} \tag{132}$$

with M^* the density of electronic excited molecules and N is the cooling gas.

To approximate the progression between the initial vibrational distribution and the equilibrium distribution, we describe the vibrational population in a simplified model. Assume the population density of the electronic state to consist of two terms

$$M^*(v) = M_S^*(v) + M_T^*(v) \tag{133}$$

where the $M_S^*(v)$ states have an average vibration number $\bar{v}$ and are distributed according to the photoexcited source, and $M_T^*(v)$ is a Boltzmann distribution (more exactly a Trainor distribution) at temperature T_V. Note that M_S^* and M_T^* are limiting cases for vibrationally unrelaxed states and totally relaxed vibrational states, respectively. Each loss from M_S^* through V-V collision is a gain to M_T^* and requires $\bar{v}$ vibration changes to completely relax as follows

$$\frac{dM_S^*}{dt} = S_1 M - Q_S M_S^* - A_e M_S^* - \bar{v}^{-1} K_{VV} M_S^* M^* - \bar{v}^{-1} K'_{VV} M_S^* N \tag{134}$$

$$\frac{dM_T^*}{dt} = \bar{v}^{-1} K_{VV} M_S^* M^* + \bar{v}^{-1} K'_{VV} M_S^* N - Q_T M_T^* - A_e M_T^* \tag{135}$$

where A_e is the Einstein coefficient for the electronic state, Q_S and Q_T are the electronic quenching rates, and S_1 is the excitation rate. The rate equation for the total electronic excited population is

$$\frac{dM^*}{dt} = S_1 M - QM^* - A_e M^* \tag{136}$$

with

$$Q_S \approx Q_T \approx Q = (Q_S + Q_T)/2 .$$

We now desire a description of the vibrational levels of the electronically unexcited states.

Spontaneous decay of the upper electronic state is governed by the Franck-Condon principle. The radiative transition from the lowest vibrational level of the electronically excited state is shown in figure 4 as the solid vertical lines in the figure. The transition in this case occurs most often at the most probable nuclear separation as determined by the

peak of the $v = o$ vibrational wave function of the upper electronic state. The most probable vibrational quantum number is determined by the most probable nuclear separation of the upper state corresponding to the middle-vertical-solid line in figure 4 with $\bar{v} \approx 9$. The range of vibrational levels of the lower electronic state populated by transitions from the lower vibrational level of the upper electronic state is determined by the uncertainty in nuclear separation of the state from which the transition was made as noted by the two remaining vertical-solid lines in figure 4 for which $\Delta v \approx 4$. Transitions from higher vibrational levels of the upper electronic state mostly occur near the classical turning points but are otherwise similar to transitions from the lowest vibrational level discussed above. The vibrational levels populated after the transition are determined by the nuclear separation appropriate to the vibrational level from which the transition was made.

If $M_S^\dagger$ represents the vibrating levels reached by radiative decay of the M_S^* states and if $M_T^\dagger$ is similarly related to M_T^*, then

$$\frac{dM_S^\dagger}{dt} = A_e M_S^* + Q_S M_S^* - (\bar{v}_S - \bar{v}_T)^{-1} K_{vv}'' \, M M_S^\dagger \tag{138}$$

$$\frac{dM_T^\dagger}{dt} = A_e M_T^* + Q_T M_T^* + (\bar{v}_S - \bar{v}_T)^{-1} K_{vv}'' \, M M_S^\dagger - \bar{v}_T^{-1} K_{vv}'' \, M M_T^\dagger \tag{139}$$

where quenching is assumed governed by the Franck-Condon principle and vibrational relaxation is treated in the same manner as for the electronic states. The starting gas is regained due to vibrational relaxation as follows

$$\frac{dM}{dt} = \bar{v}_T^{-1} \, K_{vv}'' \, M_T^\dagger \; M - S_1 M \tag{140}$$

which balances the losses due to photoexcitation.

Steady State Solution

Consider now the constant illumination of the gas and steady state conditions. Setting all derivatives of equations (134) through (140) equal to zero, and taking all densities as summed over appropriate vibrational levels, we now solve the resulting algebraic equations. First note from equation (136) that

$$M^* = \frac{S_1 M}{A_e + Q} \tag{141}$$

so that equations (134) and (135) yield

$$M_S^* = \frac{S_1 M}{A_e + Q + \bar{\upsilon}^{-1} K_{vv} M^* + \bar{\upsilon}^{-1} K'_{vv} N} \tag{142}$$

$$M_T^* = \frac{(\bar{\upsilon}^{-1} K_{vv} M^* + \bar{\upsilon}^{-1} K'_{vv} N)}{A_e + Q + \bar{\upsilon}^{-1} K_{vv} M^* + \bar{\upsilon}^{-1} K'_{vv} N} M^* \tag{143}$$

It follows equations (138) and (139) that

$$M_S^\dagger = \frac{(A_e + Q) M_S^*}{(\bar{\nu}_S - \bar{\nu}_T)^{-1} K''_{vv} M} \tag{144}$$

$$M_T^\dagger = \frac{S_1}{\bar{\nu}_T^{-1} K''_{vv}} \tag{145}$$

where the total quenching rate is

$$Q = qM + q_N N. \tag{146}$$

We now consider the requirements for an inversion on specific transitions.

Requirements for an Inversion

In order to have an inversion, we require that

$$\Delta M_S(\nu) = M_S^*(\nu) - M_S^\dagger(\nu) > 0 \tag{147}$$

or

$$\Delta M_T(\nu) = M_T^*(\nu) - M_T^\dagger(\nu) > 0 \tag{148}$$

Alternately, we may consider the ratios of the previously derived steady state solutions

$$\frac{M_S^*}{M_S^\dagger} = \frac{(\bar{\nu}_S - \bar{\nu}_T)^{-1} K''_{vv} M}{A_e + Q} > 1 \tag{149}$$

and

$$\frac{M_T^*}{M_T^\dagger} = \frac{\bar{v}_T^{-1} K_{vv}'' M}{A_e + Q} \quad \frac{\bar{v}^{-1} K_{vv} M^* + \bar{v}^{-1} K_{vv}' N}{A_e + Q + \bar{v}^{-1} K_{vv} M^* + \bar{v}^{-1} K_{vv}' N} > 1. \qquad (150)$$

First, consider the gain for a strong dipole transition ($A_e \approx 10^8$ sec^{-1}). A strong quencher at 30 Torr gives

$$Q \approx 10^{-1} \times 5 \times 10^{-10} \times 10^{18} = 5 \times 10^7 \text{ sec}^{-1} \qquad (151)$$

leading to

$$\frac{M_S^*}{M_S^\dagger} = \frac{10^{-1} \times 10^{-1} \times 5 \times 10^{-10} \times 10^{18}}{10^8 + Q} \approx 5 \times 10^{-2} \qquad (152)$$

which is nearly independent of the quenching rate Q. Clearly, the $M_T^*/M_T^\dagger$ ratio is even smaller. If the electronic state is metastable, then

$$\frac{M_S^*}{M_S^\dagger} = \frac{(\bar{v}_S - \bar{v}_T)^{-1} K_{vv}}{q} \quad \frac{Z_{E-T}}{\bar{v}_S Z_{v-v}} \qquad (153)$$

so that

$$10^{-2} \leq \frac{M_S^*}{M_S^\dagger} \leq 10^4 \qquad (154)$$

the upper limit resulting from a system with little quenching and a permanent dipole moment for V-V relaxation. Without the permanent dipole moment, then

$$10^{-2} \leq \frac{M_S^*}{M_S^\dagger} \leq 10^2. \qquad (155)$$

In most cases, $M^* \ll M \approx N$ so that for large vibrational relaxation rates (i.e., $\tau_N = \bar{v}^{-1} K_{vv} N$) for the excited levels

$$\lim_{\tau_N \to \infty} \left(\frac{M_T^*}{M_T^\dagger}\right) \sim \frac{M_S^*}{M_S^\dagger} \qquad (156)$$

requiring efficient V-V transfer to the N vibrational levels. Otherwise

$$\frac{M_T^*}{M_T^\dagger} \ll \frac{M_S^*}{M_S^\dagger} \tag{157}$$

and inversion on M_T^* ($\nu = 0$) is unlikely at pressures of 30 Torr and below.

Gain Requirements

We further simplify the equations to study the gain. The electronically excited state density is

$$M^* = S_1 M/(A_e + qM + q_N N) \tag{158}$$

and the lower level density is

$$M^\dagger \approx S_1 M/\bar{v}^{-1} K_{vv} M \tag{159}$$

giving an inversion of

$$M^* - M \approx S_1 \left(\frac{M}{A_e + qM} - \frac{1}{\bar{v}^{-1} K_{vv}'} \right)$$

$$\approx S_1 \left(\frac{1}{q} - \frac{1}{\bar{v}^{-1} K_{vv}'} \right)$$

$$\approx S_1/q. \tag{160}$$

Consider an excited molecule whose lifetime is long compared to a slow quenching rate as

$$A_e \leq qM \leq 5 \times 10^4 \text{ sec}^{-1} \tag{161}$$

which satisfies the requirement that

$$N_{E-T} >> \bar{v} N_{v-v} \approx 10^3. \tag{162}$$

The corresponding quenching rate coefficient is

$$q \leq 5 \times 10^{-14} \text{ cm}^3/\text{sec} \tag{163}$$

which is a slow quencher. Such a system forms an inversion; we now calculate the gain.

The stimulated emission cross section is

$$\sigma_e = \frac{\lambda_e^4 A_e}{4\pi^2 c \Delta\lambda_e} \tag{164}$$

where $\Delta\lambda_e$ is the emission bandwidth. For typical E-V molecular transitions

$$\Delta\lambda_e \approx 100\text{Å} = 10^{-6}\ \text{cm} \tag{165}$$

(this parameter needs further study). Consider emission around 1 μ so that

$$\alpha = \frac{\lambda_e^4 A_e}{4\pi^2 c \Delta\lambda_e} \quad \frac{S_1 M}{A_e + qM}$$

$$= \frac{3.3 \times 10^{-8} C \lambda_e^4}{4\pi^2 c \Delta\lambda_e} \quad M \quad \frac{A_a A_e}{A_e + qM}$$

$$\approx 2.7 \times 10^{-12} C \frac{A_a A_e}{A_e + qM} \quad (\text{cm}^{-1}). \tag{166}$$

If $A_a \approx A_e \approx qM \approx 10^4$, we get

$$\alpha = 2.7 \times 10^{-5}/\text{cm} \tag{167}$$

for $C = 10^3$. It is clear therefore, that the typical bandwidths of molecular E-V transitions preclude solar pumping with sufficient gain for laser operations. However, unusually narrow-band molecular metastable systems may yet prove to be viable candidates.

KINETIC MODEL OF A PHOTODISSOCIATION LASER

It is clear that the most promising systems are broadband absorbers in order to efficiently pump large volumes and narrow band emitters in order to assure high gain. This indicates that photodissociation is the most likely system with lasing from atomic excited states (probably metastables). High quantum efficiencies will require lasing to the atomic ground state with chemical dumping of the lower level. The kinetic limits for such systems will now be considered. The initial photodissociation is illustrated in figure 5.

The rate equations for photodissociation of M into A + B* are now considered so that

$$\frac{dM}{dt} = -S_1 M + K_r AB + K_r^* AB^* \tag{168}$$

where the recombination rate coefficients K_r and K_r^* are pressure-dependent if A and B are atomic species or A is at most a simple molecule. Otherwise, K_r and K_r^* is an effective two-body coefficient independent of gas pressure (ref. 33). The following also apply

$$\frac{dB^*}{dt} = S_1 M - K_r^* AB^* - QB^* - A_B B^* \tag{169}$$

$$\frac{dB}{dt} = QB^* + A_B B^* - K_r AB. \tag{170}$$

Typical values of recombination rate coefficients are $10^{-10} - 10^{-12}$, indicating from $5 \leq Z_r \leq 500$ collisions for recombination. Note that we have neglected the formation of A_2 dimers which may limit the chemical reversibility of some systems. In steady state, we have

$$(Q + A_B)B^* - K_r AB = 0 \tag{171}$$

with $A = B + B^*$ yields

$$B = \frac{\left[(K_r B^*)^2 + 4K_r(Q + A_B)B^*\right]^{\frac{1}{2}} - K_r B^*}{2K_r}. \tag{172}$$

We first note that the assumption

$$4(Q + A_B) > > K_r B^* \tag{173}$$

implies

$$A \approx B >> B^* \tag{174}$$

for which there can be no inversion. Therefore, we must require

$$K_r B^* >> 4(Q + A_B) \tag{175}$$

for which

$$B \approx \frac{A_B + Q}{K_r} << B^* \approx A \tag{176}$$

so that inversion is now possible. It follows then that

$$\frac{dB^*}{dt} \approx S_1 M - K_r^* B^{*2} - (Q + A_B)B^* \tag{177}$$

for which

$$B^* \approx \frac{[(Q + A_B)^2 + 4K_r^* S_1 M]^{\frac{1}{2}} - (Q + A_B)}{2K_r^*}. \tag{178}$$

At low power levels defined by

$$4K_r^* S_1 M << (Q + A_B)^2 \tag{179}$$

we obtain

$$B^* \approx S_1 M/(Q + A_B). \tag{180}$$

At high power levels defined by

$$4K_r^* S_1 M >> (Q + A_B)^2 \tag{181}$$

we obtain

$$B^* \approx \sqrt{\frac{S_1 M}{K_r^*}}. \tag{182}$$

Consider the gain at low power levels as given by

$$\alpha = \frac{\lambda^2 A_B}{4\pi^2 \Delta\nu} \frac{S_1 M}{Q + A_B}$$

$$= 8.4 \times 10^{-8}\, C\, \frac{A_a A_B}{Q + A_B} \tag{183}$$

so that threshold is easily achieved for $A_a \approx 10^3\ \text{sec}^{-1}$ and $A_B \approx Q$. Consider now the high power limit for which

$$B^* = \left[\frac{3.3 \times 10^{-18} C A_a M}{K_r^*}\right]^{\frac{1}{2}}$$

$$\approx 10^{11} \sqrt{CA_a} \tag{184}$$

so that

$$\alpha = \frac{\lambda^2 A_B}{4\pi^2 \Delta\nu} B^*$$

$$\approx 2.5 \times 10^{-7}\ A_B \sqrt{CA_a} \tag{185}$$

for which the threshold is easily achieved.

The main requirement for photodissociation pumping is that an inversion be formed which in turn requires

$$K_r B^* > > Q + A_B. \tag{186}$$

Using typical values for $K_r B^*$ as

$$(10^{-11})\ (10^{14}) > > Q + A_B. \tag{187}$$

Hence

$$10^3 > > Q + A_B \tag{188}$$

so that B^* is an atomic metastable not easily quenched by the starting gas. The perfluoroalkyliodides are one such example.

CONCLUSION

The present survey of gas properties through kinetic models has identified critical gas parameters for use in choosing appropriate gas combinations for solar-pumped lasers. Broadband photoabsorption in the visible or near-UV range is required to excite large volumes of gas and to ensure good solar-absorption efficiency. The photoexcitation density is independent of the absorption bandwidth. The state excited must be a metastable state which is not easily quenched by the parent gas. The emission bandwidth must be less than ~10Å to ensure lasing threshold over reasonable gain lengths. The system should show a high degree of chemical reversibility and insensitivity to increasing temperature. Other properties such as good quantum efficiency and kinetic efficiency are also implied. Although photoexcitation of electronic-vibrational transitions is considered as a possible system if the emission bands are sufficiently narrow, it appears that photodissociation into atomic metastables is more likely to result in a successful solar-pumped laser system.

Langley Research Center
National Aeronautics and Space Administration
Hampton, VA 23665
September 2, 1980

REFERENCES

1. Coneybear, J. F.: The Use of Lasers for the Transmission of Power. Radiation Conversion in Space, K. H. Billman, ed., Progress in Astronautics and Aeronautics, vol. 61, 1978, p. 279.

2. Rather, J. D. G.: New Candidate Lasers for Power Beaming and Discussion of Their Applications. Radiation Conversion in Space, K. H. Billman, ed., Progress in Astronautics and Aeronautics, vol. 61, 1978, p. 313.

3. Young, C. G.: A Sun-Pumped CW One-Watt Laser. Applied Optics, vol. 5, no. 6, 1966, pp. 993-997.

4. Wilson, J. W.; and Lee, J. H.: Modeling of a Solar-Pumped Iodine Laser. Va. J. of Science, vol. 30, no. 2, Summer 1979, p. 44.

5. Lee, J. H.; Shiu, Y. J.; and Weaver, W. R.: Direct Solar-Pumped Lasers. 1980 IEEE Region 3 Conference, Nashville, TN, April 13-16, 1980.

6. Hodgman, C. D. (Ed.): Handbook of Chemistry and Physics. Chemical Rubber Publication, Cleveland, OH, 1957, p. 3131.

7. Herzfeld, K. F.; and Litovitz, T. A.: Absorption and Dispersion of Ultrasonic Waves. Academic Press, 1959, chapters VI and VII.

8. Massey, H. S. W.: Atomic and Molecular Collisions. Halsted Press, New York, 1979, chapter 8.

9. Bamford, C. H.; and Tipper, C. F. H. (Ed.): Comprehensive Chemical Kinetics, vol. 3, chapter 4. Elsevier Press, 1969.

10. McDaniel, E. W., et. al.: Compilation of Data Relevant to Nuclear-Pumped Lasers. Redstone Arsenal, AL Technical Report H-78-1, December 1978.

11. Hofman, H.; and Leone, S. R.: Collisional Deactivation of Laser-Excited $Br^*(^2P_{1/2})$ Atoms with Halogen and Interhalogen Molecules. Chem. Phys. Lett., vol. 54, no. 2., March 1978, pp. 314-319.

12. Dobychin, S. L.; Mikheev, L. D.; Pavlov, A. B.; Fakanov, V. P.; and Khondarkovskii, M. A.: Quenching of Excited Iodine Atoms $I(5^2P_{1/2})$ by Molecules with C-I Bonds. Sov. J. Quantum Electronics, vol. 8, no. 11, November 1978, pp. 1383-1384.

13. Lemont, S.; and Flynn, G. W.: Vibrational State Analysis of Electronic-to-Vibrational Energy Transfer Process. Ann. Rev. Phys. Chem., vol. 28, 1977, pp. 261-282.

14. Lin, M. C.; and Shortridge, R. G.: Electronic-to-Vibrational Energy Transfer Reactions X* + CO (X = O, I, and Br). Chem. Phys. Lett., vol. 29, no. 1, November 1974, pp. 42-49.

15. Hariri, A.; and Wittig, C.: Electronic-to-Vibrational Energy Transfer from Br ($4^2P_{1/2}$) to CO_2, COS, and CS_2. Chem. Phys., vol. 67, no. 10, November 1977, pp. 4454-4462.

16. Peterson, A. B.; and Wittig, C.: Infrared Molecular Lasers Pumped by Electronic-Vibrational Energy Transfer from Br($4^2P_{1/2}$): CO_2, N_2O, HCN, and C_2H_2. Appl. Phys. Lett., vol. 27, no. 5, September 1975, pp. 305-307.

17. Reisler, H.; and Wittig, C.: Temperature Dependence of the Quenching of Br($4^2P_{1/2}$) by CO_2 and HCl with Accompanying Vibrational Excitation. J. Chem. Phys., vol. 68, no. 1, April 1978, pp. 3308-3309.

18. Fisher, E. R.; and Smith, G. K.: Vibrational-Electronic Coupling in the Quenching of Electronically Excited Alkali Atoms by Diatomics. Appl. Optics, vol. 10, no. 8, August 1971, pp. 1803-1813.

19. Zipf, E. C.: The Collisional Deactivation of Metastable Atoms and Molecules in the Upper Atmosphere. Canadian J. Chem., vol. 47, 1969, pp. 1863-1870.

20. Bekefi, G., ed.: Principles of Laser Plasmas. John Wiley Pub., New York, 1976, Chapter 5.

21. Jeffers, W. Q.; and Kelley, J. D.: Calculations of V-V Transfer Probabilities in CO-CO Collisions. J. Chem. Phys., vol. 55, no. 9, November 1971, pp. 4433-4437.

22. Goldstein, H.: Classical Mechanics. Addison-Wesley Publishers, 1950, Chapter 9.

23. Sakurai, J. J.: Advanced Quantum Mechanics. Addison-Wesley Publishers, 1967, Chapters 2 and 3.

24. Messiah, A.: Quantum Mechanics, Volume II. John Wiley Pub., New York, 1966, Chapter XXI.

25. Herzberg, G.: Molecular Spectra and Molecular Structure I. Spectra of Diatomic Molecules. D. Van Nostrand, New York, 1965, Chapter I.

26. Lengyel, B. A.: Introduction to Laser Physics. John Wiley and Sons Pub., New York, 1966, Chapter I.

27. Yariv, A.: Quantum Electronics. John Wiley and Sons Pub., New York, 1975, Chapter 8.

28. Jackson, J. D.: Classical Electrodynamics. John Wiley and Sons Pub., New York, 1962, Chapter 17.

29. Merybacker, E.: Quantum Mechanics. John Wiley and Sons Pub., New York, 1963, Chapter 20.

30. Siegman, A. E.: An Introduction to Lasers and Masers. McGraw-Hill, New York, 1971, Chapter 3.

31. Herzberg, G.: Molecular Spectra and Molecular Structure I. Spectra of Diatomic Molecules. D. Van Nostrand, New York, 1965, Chapter VII.

32. Carter, J. R.; and Tada, H. Y.: Solar Cell Radiation Handbook. TRW 21945-6001-RU-00, June 1973.

33. Jordan, P. C.: Chemical Kinetics and Transport. Plenum Press, New York, 1979, Chapter 5.

Table I. Molecular Constants of Some Gases

Gas	Collision Coefficient cm^3/sec	Diameter, A	Θ_r °K
NH_3	3.5 E-10	3.06	8.5
Ar	1.5 E-10	2.92	--
CO	2.0 E-10	3.16	2.7
CO_2	2.4 E-10	3.28	0.8
He	1.7 E-10	2.27	--
H_2	3.8 E-10	2.37	85
N_2	2.0 E-10	3.30	2.8
O_2	1.7 E-10	2.95	2.5

Table II. Rotational Relaxation

Gas	Z_{R-T}	Θ_r, °K
H_2	343	85
D_2	208	43
N_2	5.1	2.8
O_2	23.5	2.5

Table III. Characteristic Vibrational Temperatures and Relaxation Number

Gas	Θ_v°K	Z_{V-T}
N_2	3336	3.5 E+7
O_2	2228	2.0 E+7
Cl_2	812	3.4 E+3
CO	3080	8.3 E+8
CO_2	2000*	5 E+4
COS	1400*	1 E+4
CS_2	1000*	8 E+3

*Average value of three modes.

Table IV. Vibrational Relaxation in Gas Mixtures (Z_{V-T})

	H_2	He	Ar	O
O_2	2.9 E+4	------	1.9 E+6	-------
CO	5.5 E+5	1.8 E5	3.5 E+8	8.8 E+3

	N_2O	CO_2	H_2O
N_2O	7.5 E+3	-------	1.1 E+2
CO_2	-------	5.7 E+4	1.1 E+2

Table V. Spin-Orbit Relaxation Data (ref. 9) - Z_{E-RT}

						ΔE (eV)	Z_{E-RT}
$Se(4^3P_0)$	+	Ar	→	$Se(4^3P_1)$	+	Ar	.065	8.3 E+3
$Se(4^3P_0)$	+	H_2	→	$Se(4^3P_1)$	+	H_2	.065	1.0
$Se(4^3P_0)$	+	O_2	→	$Se(_4{}^3P_1)$	+	O_2	.065	1.3 E+2
$Cs(6^2P_{3\ 2})$	+	Ar	→	$Cs(6^2P\ )$	+	Ar	.066	7.1 E+4
$Fe(a^5D_3)$	+	Ar	→	$Fe(a^5D_4)$	+	Ar	.050	1.1 E+5
$Fe(a^5D_3)$	+	H_2	→	$Fe(a^5D_4)$	+	H_2	.050	27.
$Fe(a^5D_3)$	+	D_2	→	$Fe(a^5D_4)$	+	D_2	.050	33.
$Fe(a^5D_3)$	+	He	→	$Fe(a^5D_4)$	+	He	.050	3.3 E+3
$Fe(a^5D_3)$	+	N_2	→	$Fe(a^5D_4)$	+	N_2	.050	1.0 E+3
$Fe(a^5D_3)$	+	CO	→	$Fe(a^5D_4)$	+	CO	.050	74.
$Fe(a^5D_3)$	+	Fe	→	$Fe(a^5D_4)$	+	Fe	.050	2.
$Rb(5^2P\ )$	+	Ar	→	$Rb(^5P\ )$	+	Ar	.029	4. E+3
$Ne(3^3P_0)$	+	Ne	→	$Ne(3^3P_1)$	+	Ne	.043	1. E+4
$Ne(3^3P_0)$	+	Ne	→	$Ne(3^3P_2)$	+	Ne	.093	1. E+4
$Ne(3^3P_1)$	+	Ne	→	$Ne(3^3P_2)$	+	Ne	.050	1. E+3
$K(4^2P_{3/2})$	+	Ar	→	$K(4^2P_{1/2})$	+	Ar	.007	1.5
$NO(X^2\pi_{3/2})$	+	NO	→	$NO(X^2\pi_{1/2})$	+	NO	.015	15

Table VI. Quenching of Halogen Metastables (Z_{E-RT})

	I_2	IBr	Br_2	ICl	BrCl	Cl_2
$Br(4^2P_{1/2})$	100	175	345	189	7142	8333
$I(5^2P_{1/2})$	40	100	175	345	345	1000

Table VII. Quenching of $I(5^2P_{1/2})$

Gas	Z_{E-RT}
CF_3I	6.1 E+6
C_2F_5I	9.5 E+6
$n\text{-}C_3F_7I$	1.2 E+6
$i^1\text{-}C_3F_7I$	1. E+7
$n\text{-}C_4F_9I$	2. E+5

Table VIII. Spin-Orbit to Vibration Transfer

	ΔE	$Z_{E\text{-}VRT}$
$Se(4^3P_0) + N_2O \longrightarrow Se(4^3P_1) + N_2O(\nu_2=1)$	5.4 E-3	1.6
$Se(4^3P_0) + CO_2 \longrightarrow Se(4^3P_1) + CO_2(\nu_2=1)$	1.5 E-2	1.4
$Se(4^3P_0) + CO \longrightarrow Se(4^3P_1) + CO(\nu=1)$	4.7 E-2	181.
$Se(4^3P_0) + N_2 \longrightarrow Se(4^3P_1) + N_2(\nu=1)$	2.4 E-2	67.

Table IX. Vibrational Excitation by $I(5^2P_{1/2})$

Target	Product	$Z_{E\text{-}VRT}$
H_2	$HI(v)$	2.2 E+3
D_2	$DI(v)$	1.8 E+3
HI	$HI(v)$	1.3 E+3
C_3H_8	$HI(v)$	3.3 E+3
N_2	$N_2(v)$	1 E+6

Table X. $Br(4^2P_{1/2})$ Vibrational Excitation Transfers

Dominant State	$Z_{E\text{-}VRT}$	ΔE (eV)
CO_2 (101)	13.3	-.004
HCN (001)	12.3	.045
N_2O (140)	76.9	.004
HCl (1)	43.7	.095
HF (1)	6.4	.033
HBr (1)	500.	.135

Table XI. $Na(3^2P)$ Quenching

Product	$Z_{E\text{-}VRT}$	$\Delta E(\nu)$	ν
$N_2(\nu)$	1.1	.15	7
$NO(\nu)$	1.	.09	9
$O_2(\nu)$	1.	.12	11
$CO(\nu)$	2.	.07	8
$H_2(\nu)$	2.	.21	4

Table XII. $Tl(6^2P_{3/2})$ Quenching

Gas	$Z_{E\text{-}VRT}$
O_2	1.
N_2	1.3 E+4
CO	2.7 E+3
NO	5.1

Table XIII. $O(2^1D_2)$ Transfer Rates

Gas	$Z_{E\text{-}VRT}$
N_2	4
O_2	4
NO	1.3
N_2O	1.2
H_2	1.1
CO	6.7
CO_2	10

Table XIV. Quenching for Molecular Metastables (Z_{E-VRT})

	O_2	N_2	CO	CO_2	NO
$O_2(a^1\Delta_g)$	2 E+8	5 E+8	-----	-----	4. E+6
$O_2(b^1\Sigma_g)$	4 E+5	1 E+5	7 E+4	2 E+3	33(?)
$N_2(A^3\Sigma_u)$	2 E+8	2 E+2	-----	-----	2.8

Table XV. Excitation Transfer for Ar

Molecule	Product	Z, Ar($^3P_1$)	Z, Ar($^1P_1$)
H_2	$H_2(B^1\Sigma_u)$	2.	30
N_2	$N_2(C^3\pi_u)$	20	19.
O_2	$O(2^1S) + O$	4	---
	$O(2^1D) + O$	--	1.8
CO	?	4.4	2.4
NO	?	1	---

Table XVI. Excitation Transfer for $N_2(A^3\Sigma_u)$

Molecule	Product	Z_{E-EV}
H_2	?	6.7 E+4
O_2	$O_2(B^3\Sigma_u)$	33
CH_4	?	>1.2 E+5
C_2H_2	?	1.25
C_2H_4	$C_2H_2 + H_2$	1.8
CO	$CO(a^3\pi)$	10.
NO	$NO(A^2\Sigma+)$	2.8
NH_3	$NH(A^3\pi) + N_2$	?
C_2N_2	$CN(a^3\Sigma_u) + CN$	3.2
SO_2	$SO_2(a^3B_1)$	4.4

Table XVII. Values for $CO(v) + AB \rightarrow CO(v-1) + AB(1)$

Gas(AB)	v	Z_{v-v}
CO	2	113
	3	96
	4	100
	5	140
	6	250
	7	560
	8	1130
	9	1842
	10	2917
	11	4667
O_2	1	2.6 E+6
	12	9.4 E+3
	13	4.5 E+3
N_2	1	3.9 E+4
	4	8.2 E+4
	5	1.2 E+5
	6	1.8 E+5
	7	2.4 E+5
	8	2.7 E+5
	9	4.0 E+5
	10	5.0 E+5
	11	9.0 E+5

Table XVIII. Experimental Collison Numbers for Intermolecular Vibrational Energy Transfer at 300°K

A	ν_B	ν_A (cm^{-1})	ν_B (cm^{-1})	i	$\Delta\nu$ (cm^{-1})	Z_{AB}
			Singly dispersing mixtures			
SF_6	CHClF	344	369	1	25	50
C_2H_4	C_2H_6	810	821.5	1	11.5	40
			Doubly dispersing mixtures			
CCl_2F_2	CH_3OCH_3	260	250	1	10	5
CH_3Cl	CH_3OCH_3	732	250	3	18	70
SF_6	CH_3OCH_3	344	164	2	16	80
CHF_3	C_2F_4	507	507	1	0	50
SF_6	C_2F_4	344	190	2	36	70
CF_4	C_2F_4	345	220	2	5	110
			Spectroscopic data			
$NO(A^2\Sigma+)$	N_2	2341	2330	1	11	7.9×10^3
$NO(X^2II)$	CO	1876	2143	1	267	1.0×10^4
$NO(X^2II)$	N_2	1876	2330	1	454	5.0×10^5
CO	O_2	2143	1556	1	587	4.5×10^6
$NO(X^2II)$	CH_2	1876	1534	1	342	1.1×10^3
CO	CH_4	2143	1534	1	609	3.3×10^4
$NO(X^2II)$	D_2S	1876	1892	1	16	94
$NO(X^2II)$	H_2O	1876	1595	1	281	160
$NO(X^2II)$	H_2S	1876	1290	1	586	310
$No(X^2II)$	D_2O	1876	1179	1	697	1000

Z_{AB} is the collision number for vibration-vibration transfer between one quantum of mode of frequency ν_A of molecule A and i quanta of mode of frequency ν_B of molecule B. (Frequencies are for 0-1 vibrational excitation.)

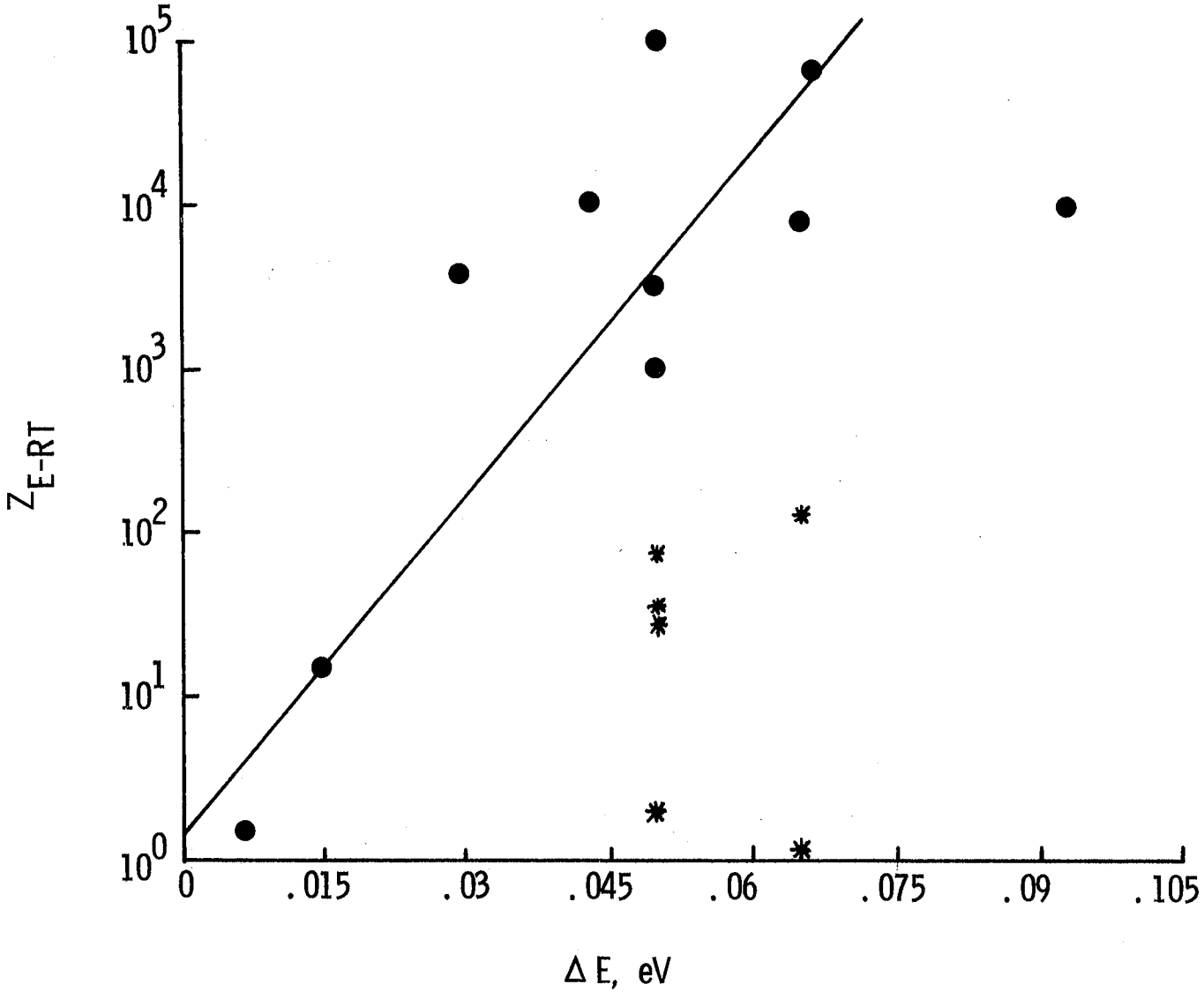

Figure 1. Relaxation of spin-orbit electronic states shown in Table V. Data shown as asterisk are molecular quenchers for which vibration modes may be excited.

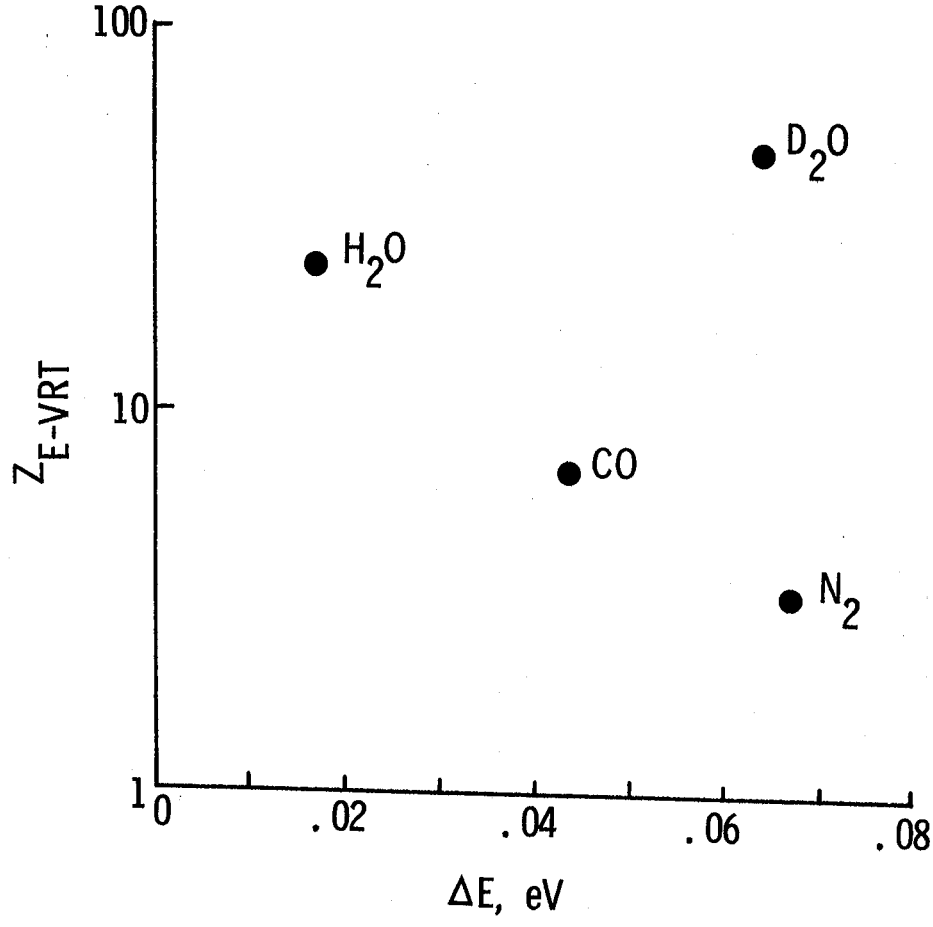

Figure 2. Spin-orbit relaxation of $Hg(6^3P_1)$ involving vibrational excitation.

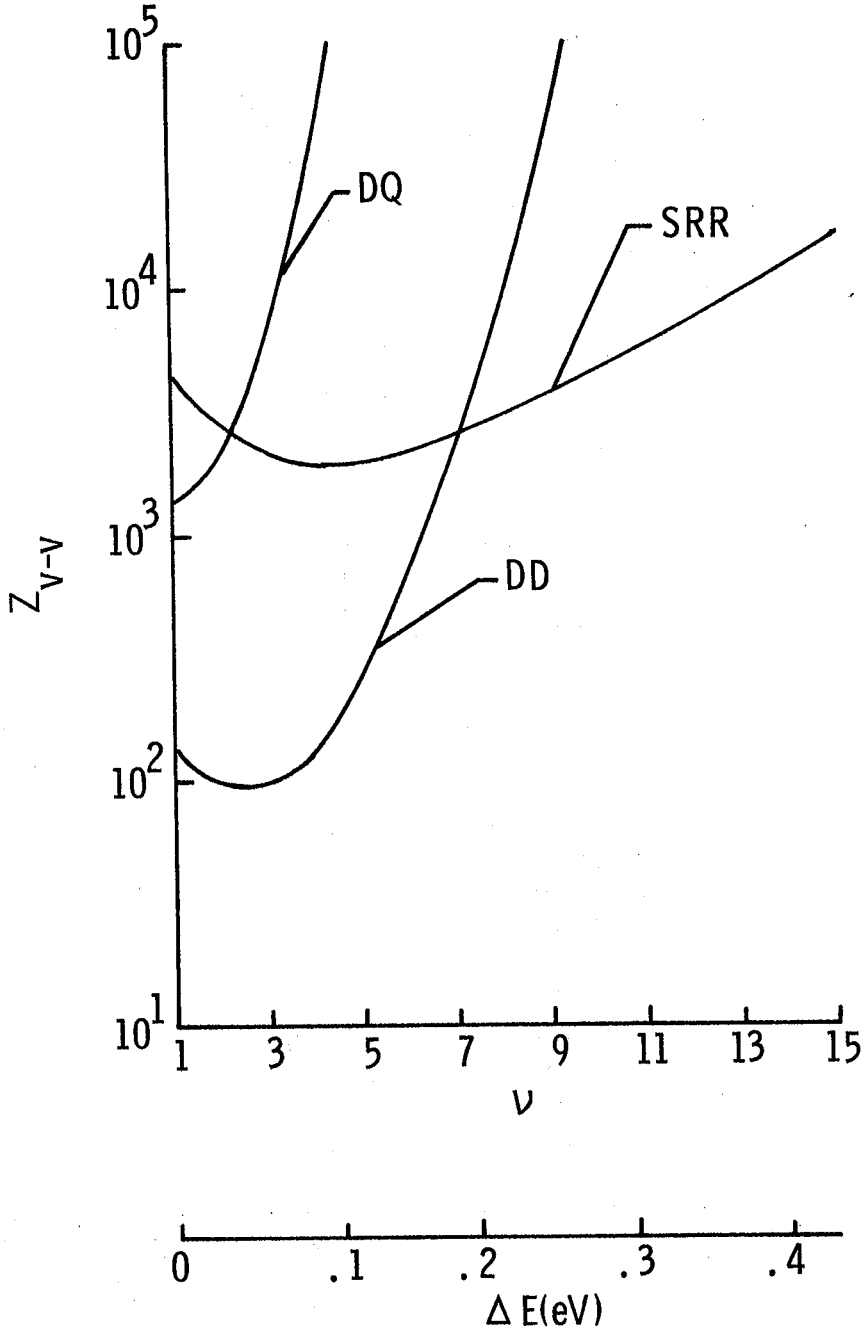

Figure 3. Collision v-v transfer rate for CO at room temperature from three contributions: DD - dipole-dipole; DQ - dipole-quadrupole; and SRR - short-range repulsion.

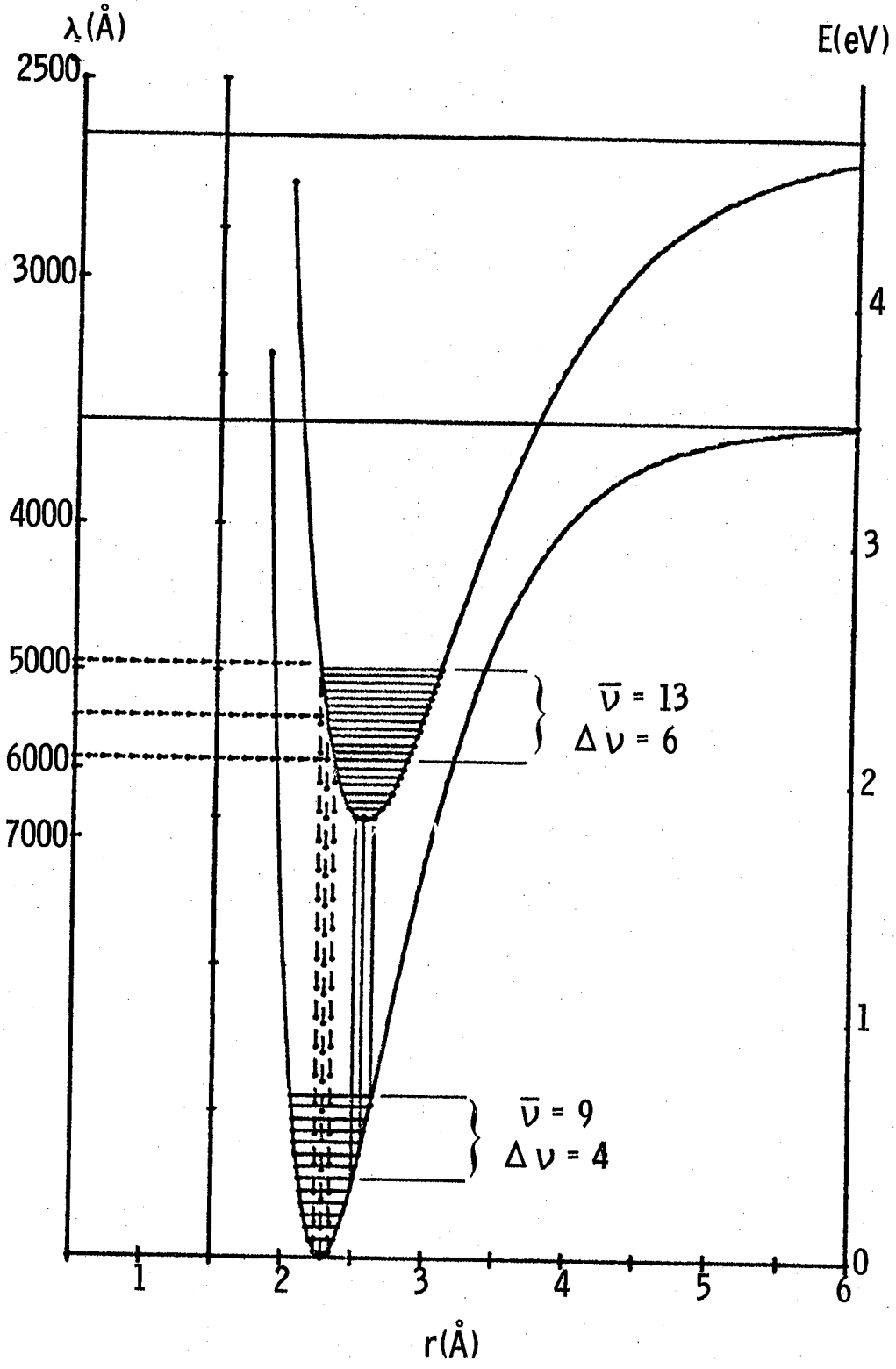

Figure 4. Photoabsorption from ground state to electronic-vibration excited state for wavelengths between 4950 A to 5900 A. Photo-emission from lowest vibrational level of electronic excited state also indicated by solid vertical lines.

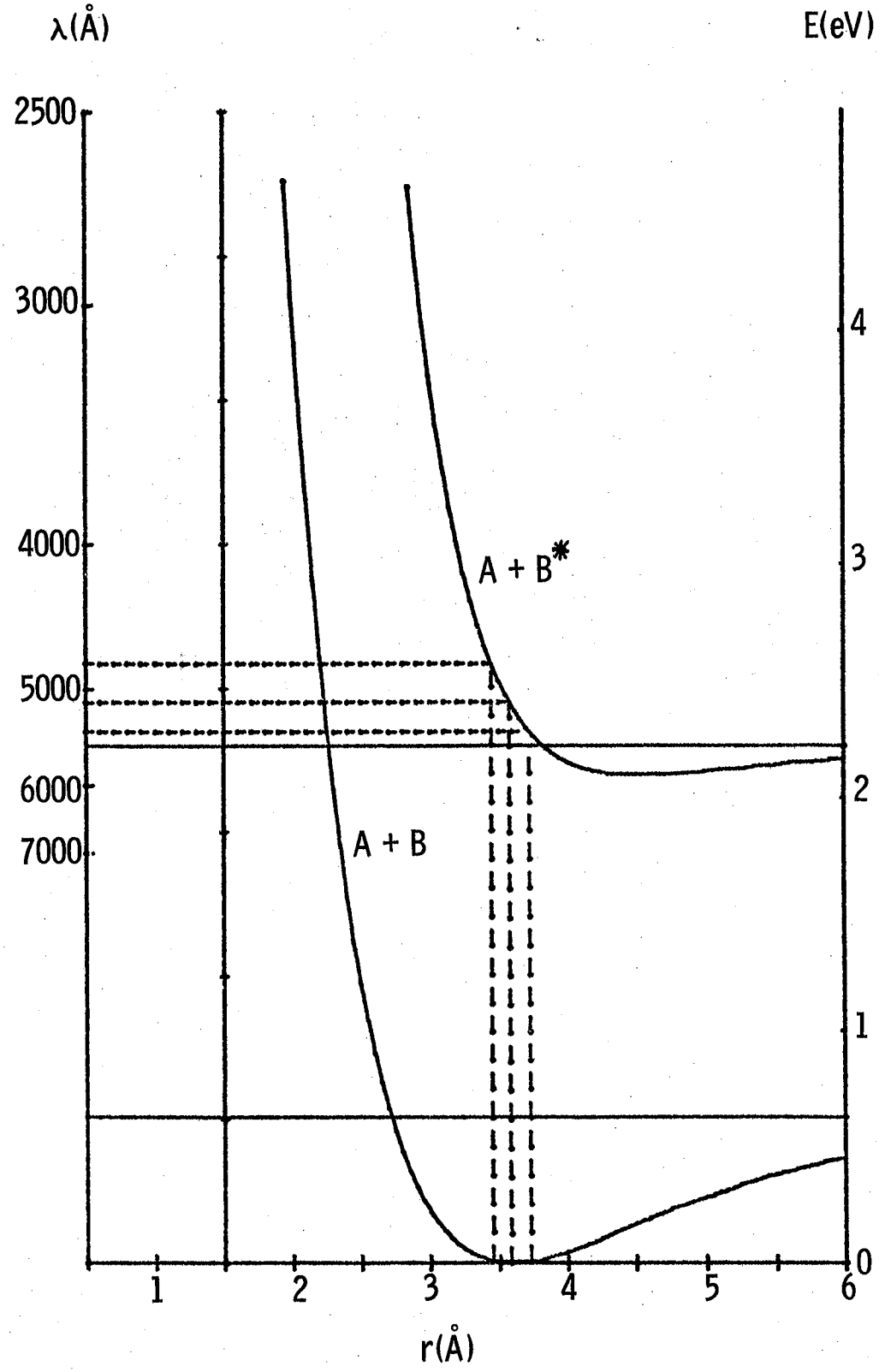

Figure 5. Photodissociation from the ground state into an unbound state in which one fragment is electronically excited.

1. Report No.	2. Government Accession No.	3. Recipient's Catalog No.
NASA TM-81894		

4. Title and Subtitle	5. Report Date
SOLAR-PUMPED GAS LASER DEVELOPMENT	December 1980
	6. Performing Organization Code
7. Author(s)	8. Performing Organization Report No.
John W. Wilson	
9. Performing Organization Name and Address	10. Work Unit No.
NASA Langley Research Center Hampton, Virginia 23665	506-55-13-07
	11. Contract or Grant No.
	13. Type of Report and Period Covered
12. Sponsoring Agency Name and Address	Technical Memorandum
National Aeronautics and Space Administration Washington, DC 20546	14. Sponsoring Agency Code

15. Supplementary Notes

Interim technical information release, subject to possible revision and/or later formal publication.

16. Abstract

High power lasers in space have potential as an effective means of space power transmission. The direct conversion of solar radiation into an inverted population for extraction in an optical cavity holds promise as a relatively simple system design when compared to other means of producing laser power through intermediate energy conversion steps. A survey of gas properties through detailed kinetic models has led to the identification of critical gas parameters for use in choosing appropriate gas combinations for solar-pumped lasers. Broadband photoabsorption in the visible or near-UV range is required to excite large volumes of gas and to insure good solar absorption efficiency. The photoexcitation density is independent of the absorption bandwidth. The state excited must be a metastable state which is not quenched by the parent gas. The emission bandwidth must be less than ~ 10 Å to insure lasing threshold over reasonable gain lengths. The system should show a high degree of chemical reversibility and an insensitivity to increasing temperature. Other properties such as good quantum efficiency and kinetic efficiency are also implied. Although photoexcitation of electronic-vibrational transitions is considered as a possible system if the emission bands are sufficiently narrow, it appears that photodissociation into atomic metastables is more likely to result in a successful solar-pumped laser system.

17. Key Words (Suggested by Author(s))	18. Distribution Statement
Solar Energy Gas Lasers Kinetics Photoprocesses	Unclassified - Unlimited Subject Category - 36

19. Security Classif. (of this report)	20. Security Classif. (of this page)	21. No. of Pages	22. Price*
Unclassified	Unclassified	64	A04

For sale by the National Technical Information Service, Springfield, Virginia 22161